Supplementary materials

The structure diversity of photoluminescent lanthanide(III) coordination compounds with an isothiazole derivative

Sanzhenakova E.A., Smirnova K.S., Pozdnyakov I.P., Berezin A.S., Potkin V.I., Lider E.V.*

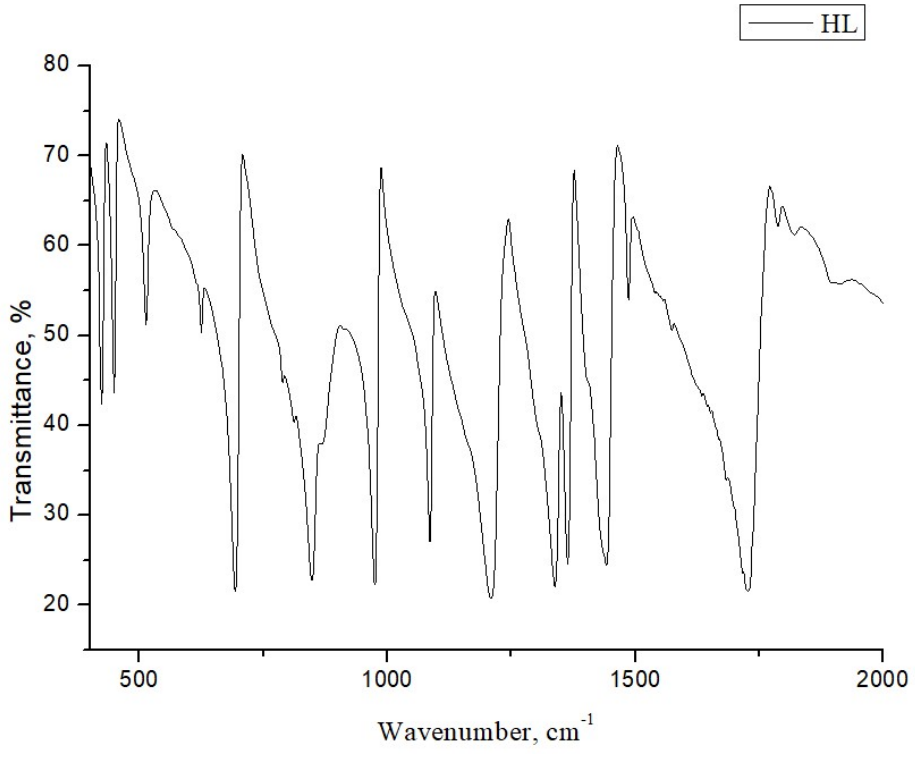

a)

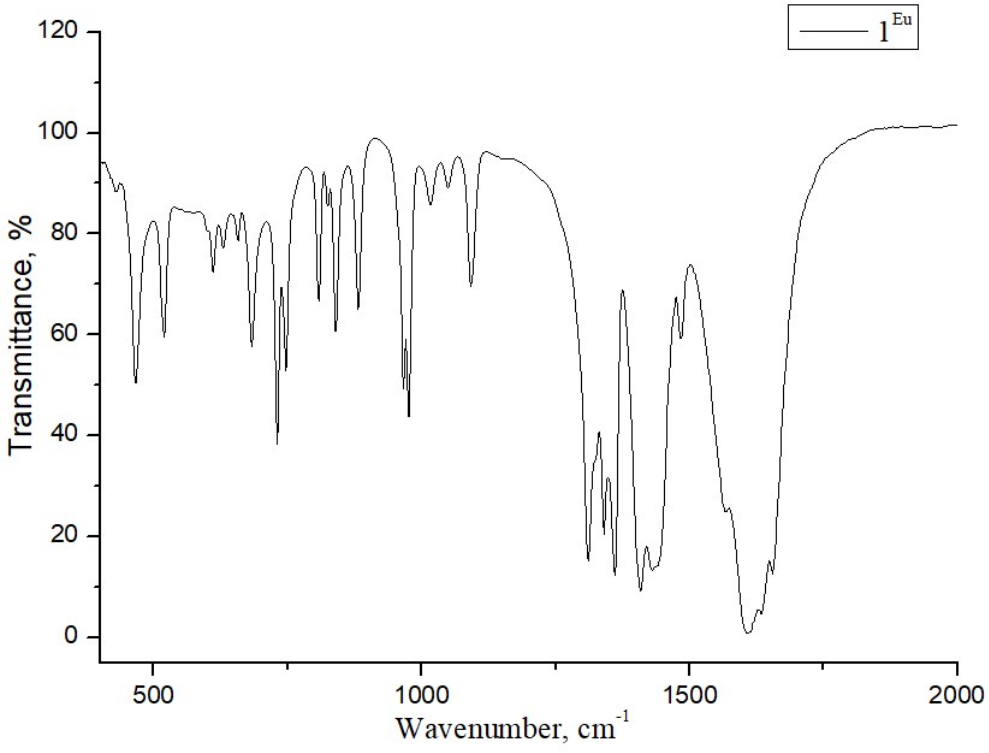

b)

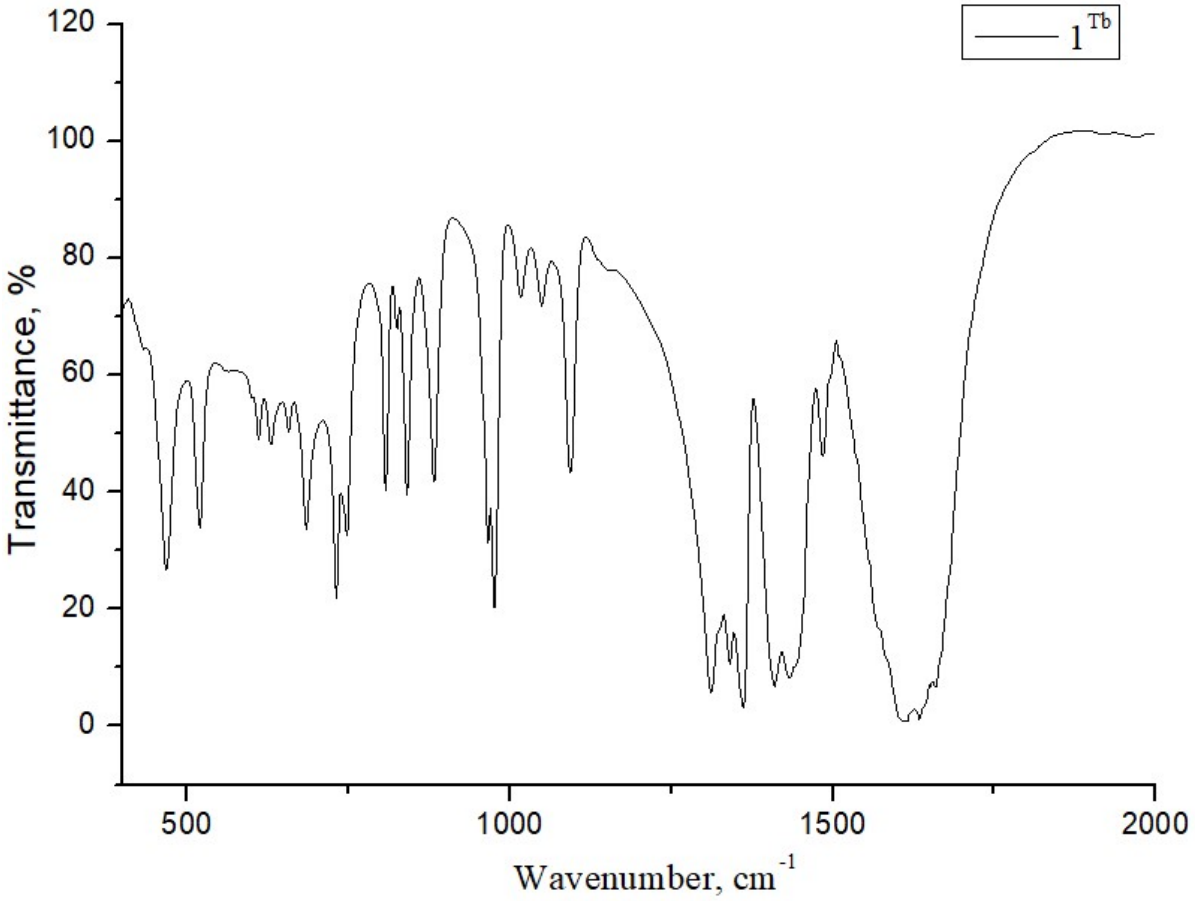
1Tb
Transmittance, %
Wavenumber, cm-1
120
100
80
60
40
20
0
500
1000
1500
2000

c)

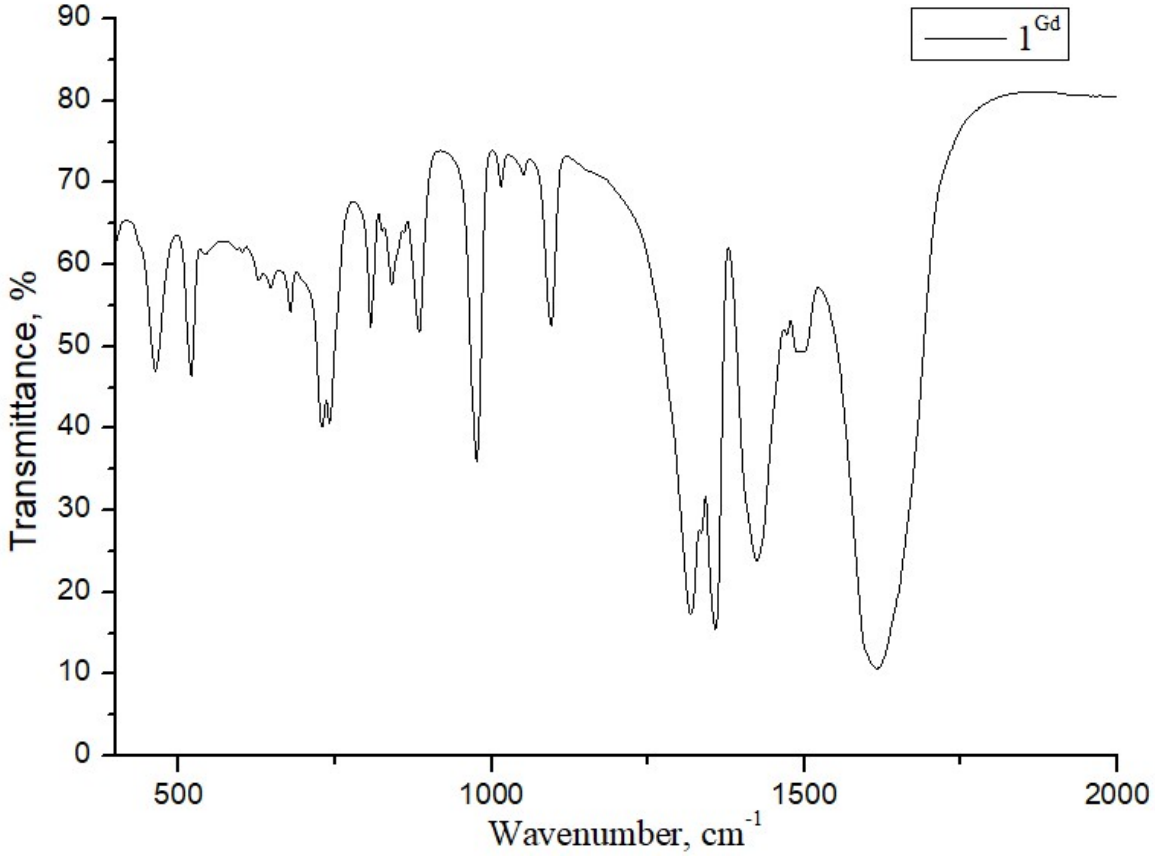
1Gd
Transmittance, %
Wavenumber, cm-1
90
80
70
60
50
40
30
20
10
0
500
1000
1500
2000

d)

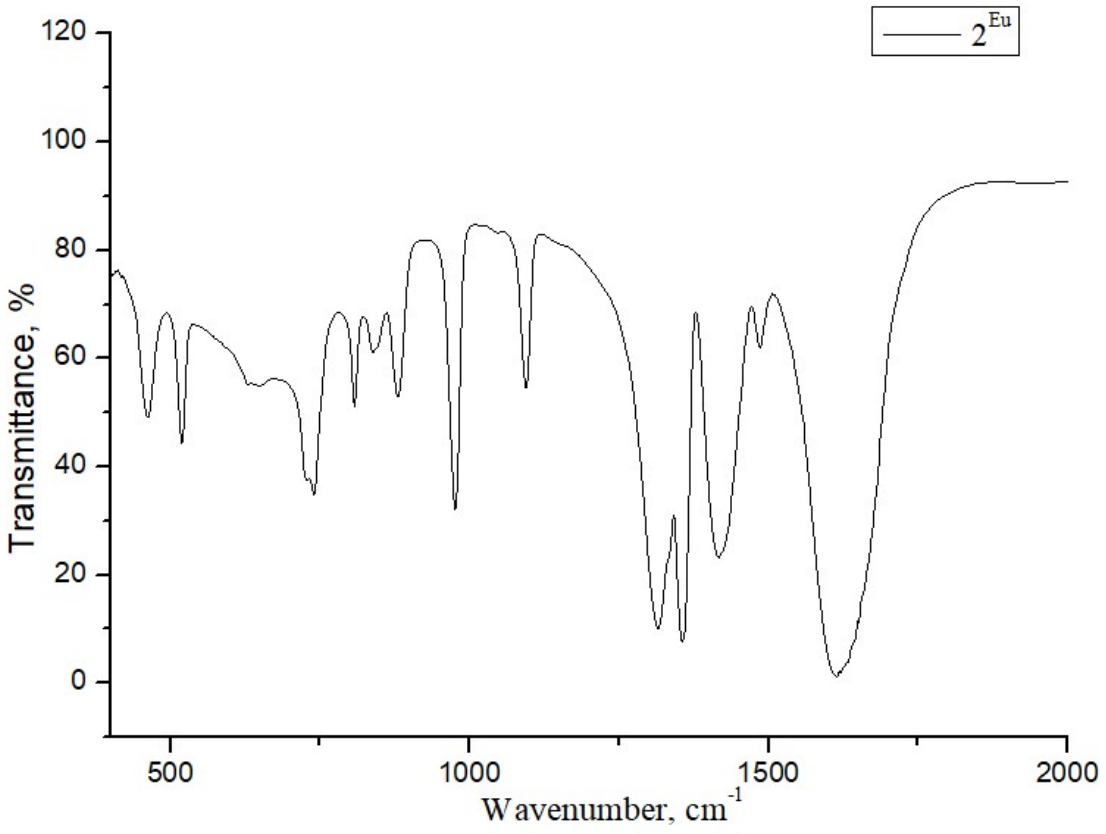
2Eu
120
100
80
60
40
20
0
Transmittance, %
500
1000
1500
2000
Wavenumber, cm-1

e)

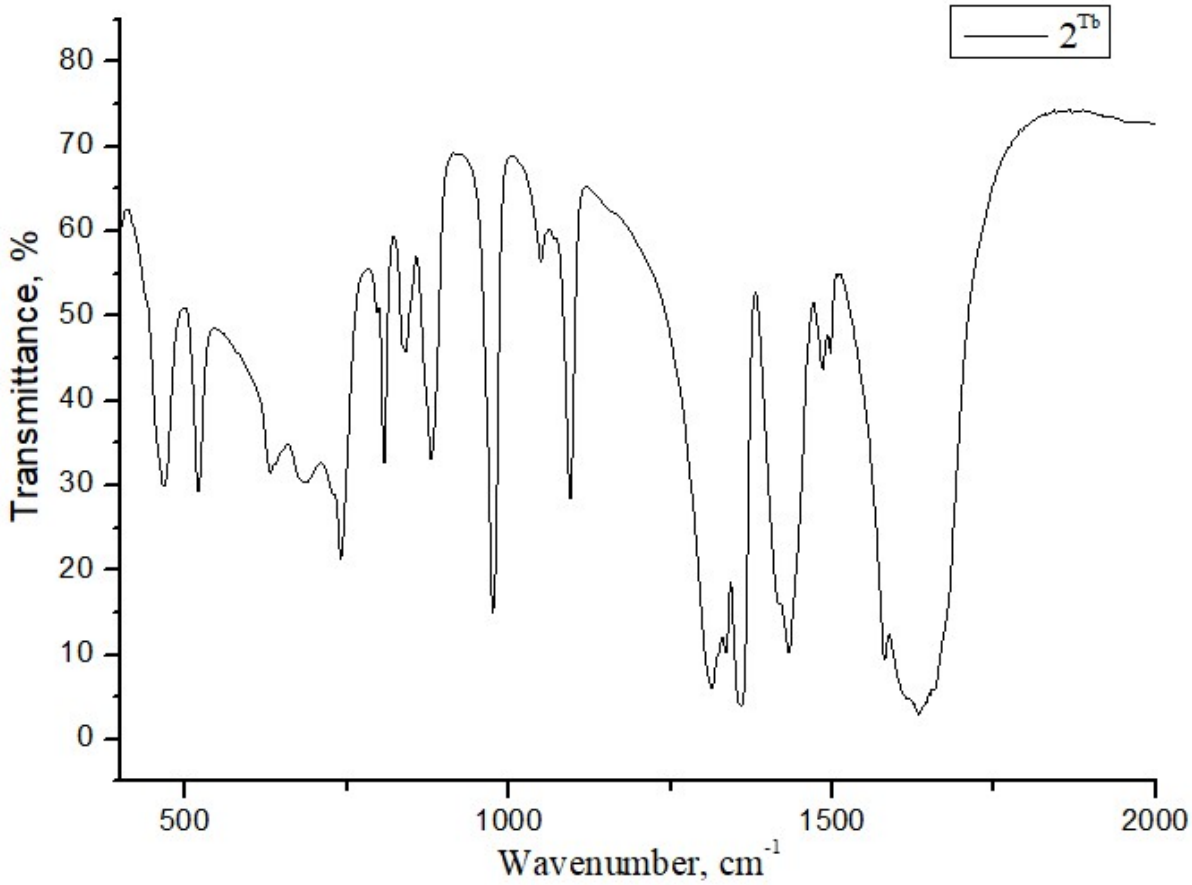
2Tb
80
70
60
50
40
30
20
10
0
Transmittance, %
500
1000
1500
2000
Wavenumber, cm-1

f)

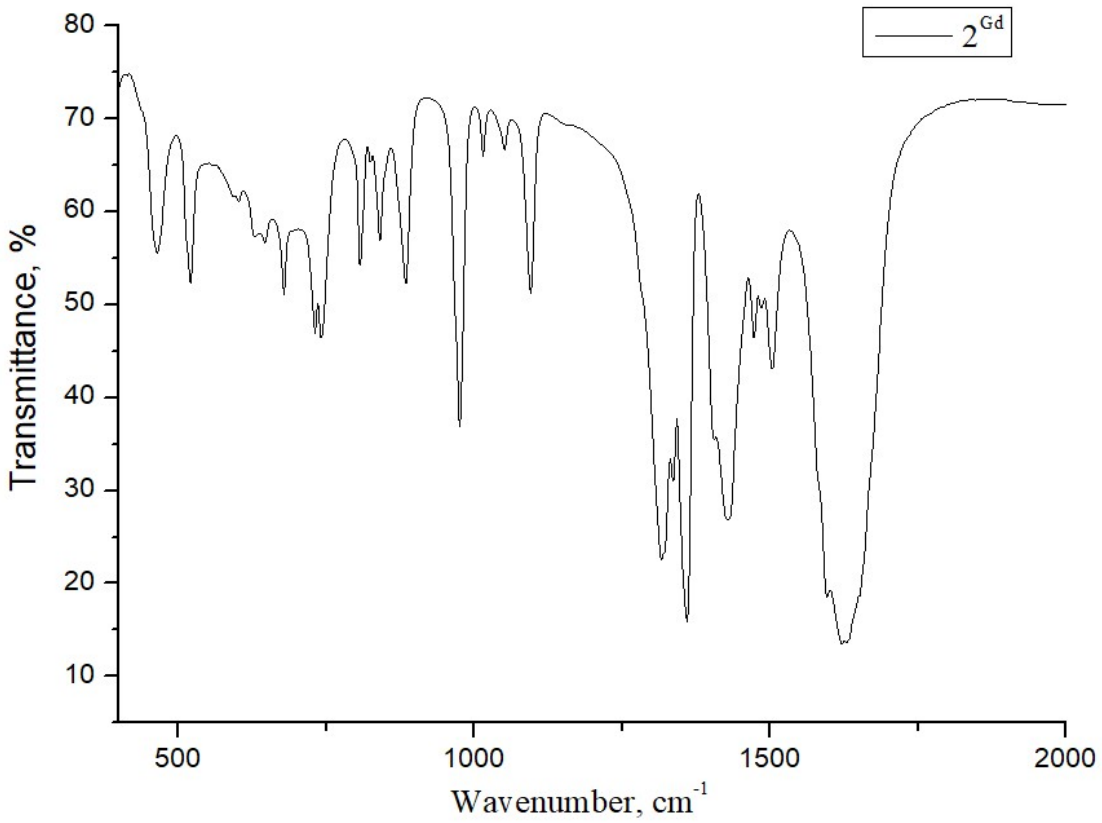

g)

Figure S1. IR spectra of the compounds in KBr.

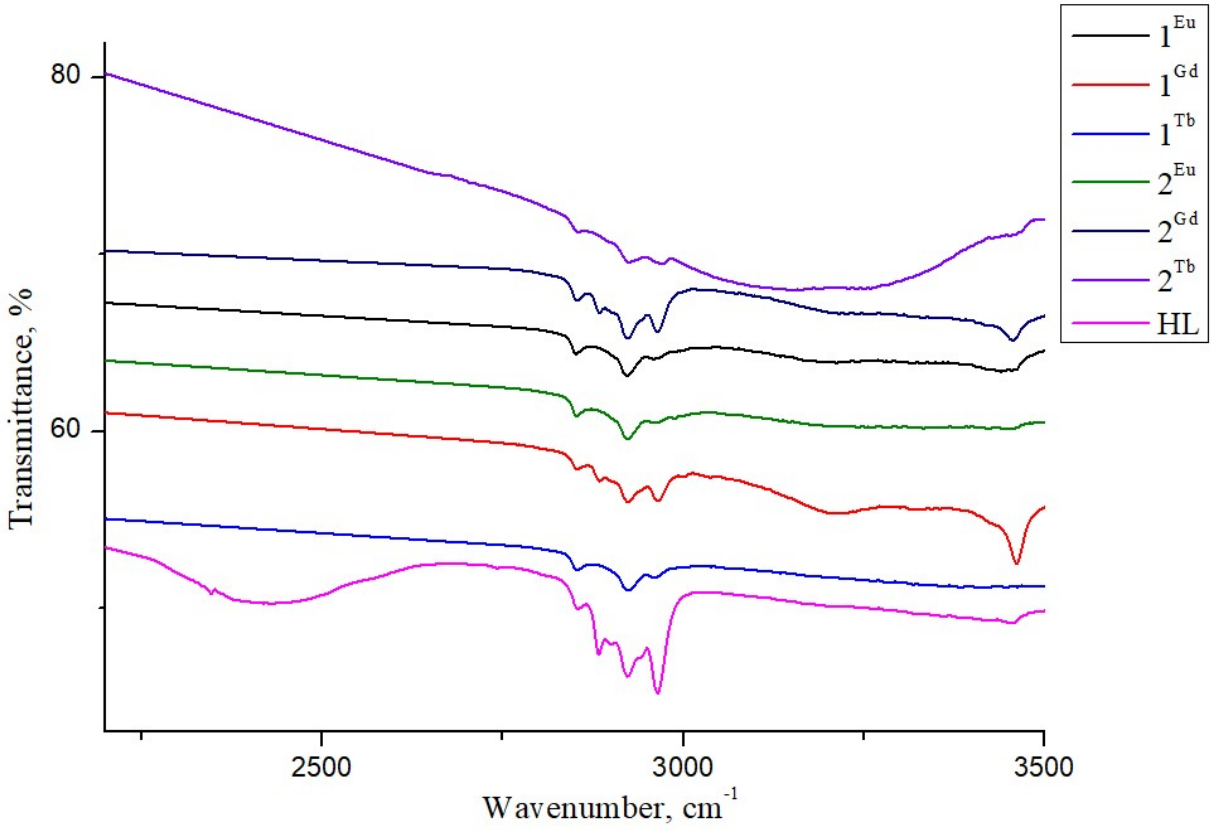

Figure S2. IR spectra of the compounds in fluorinated oil.

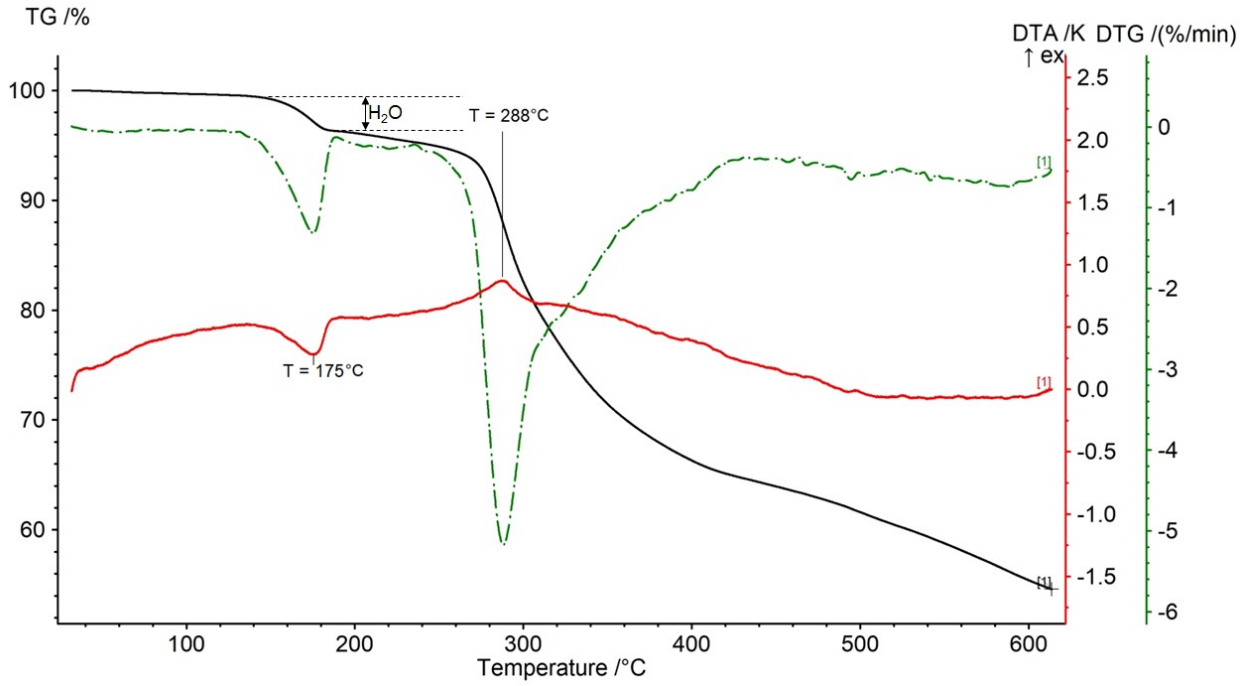

Figure S3. The thermogravimetric curve of compound $\mathbf{1}^{\mathbf{Eu}}$.

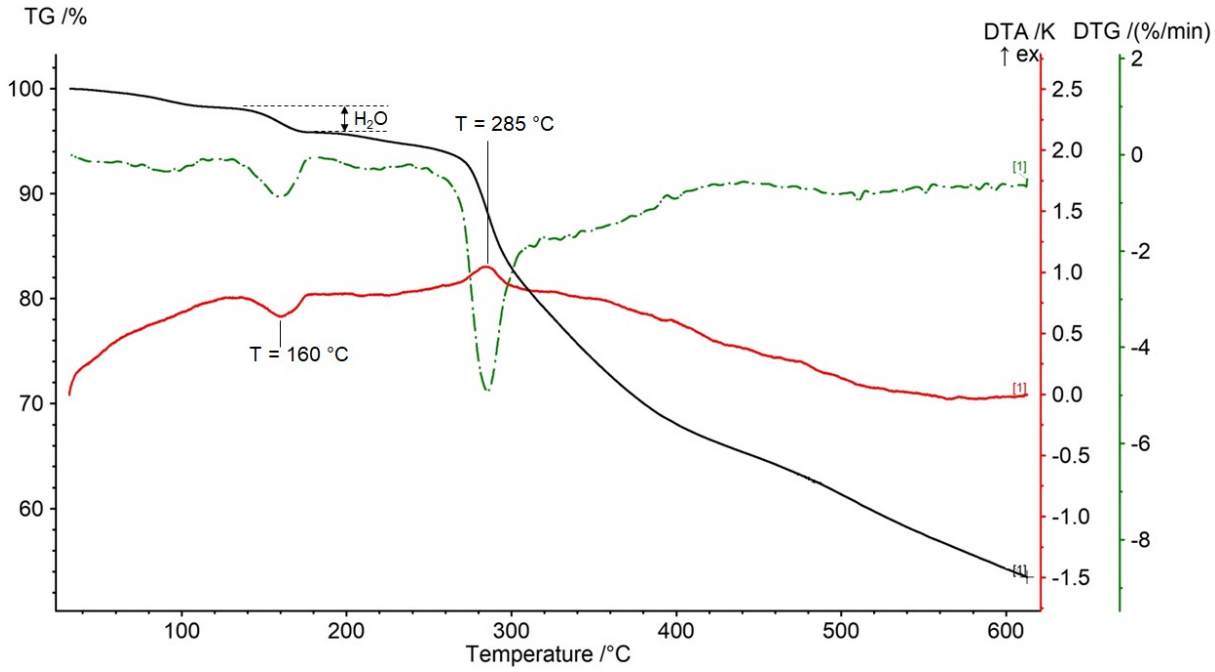

Figure S4. The thermogravimetric curve of compound $\mathbf{1}^{\mathbf{Tb}}$.

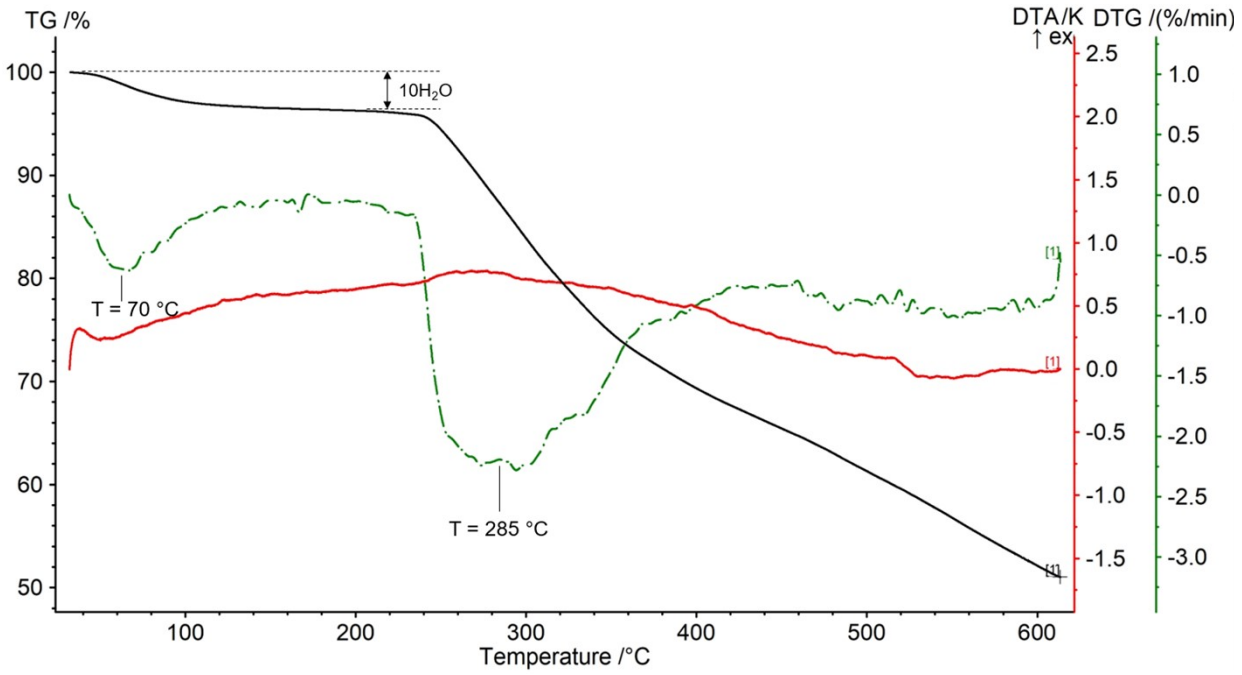

Figure S5. The thermogravimetric curve of compound $\mathbf{2}^{\mathbf{Eu}}$.

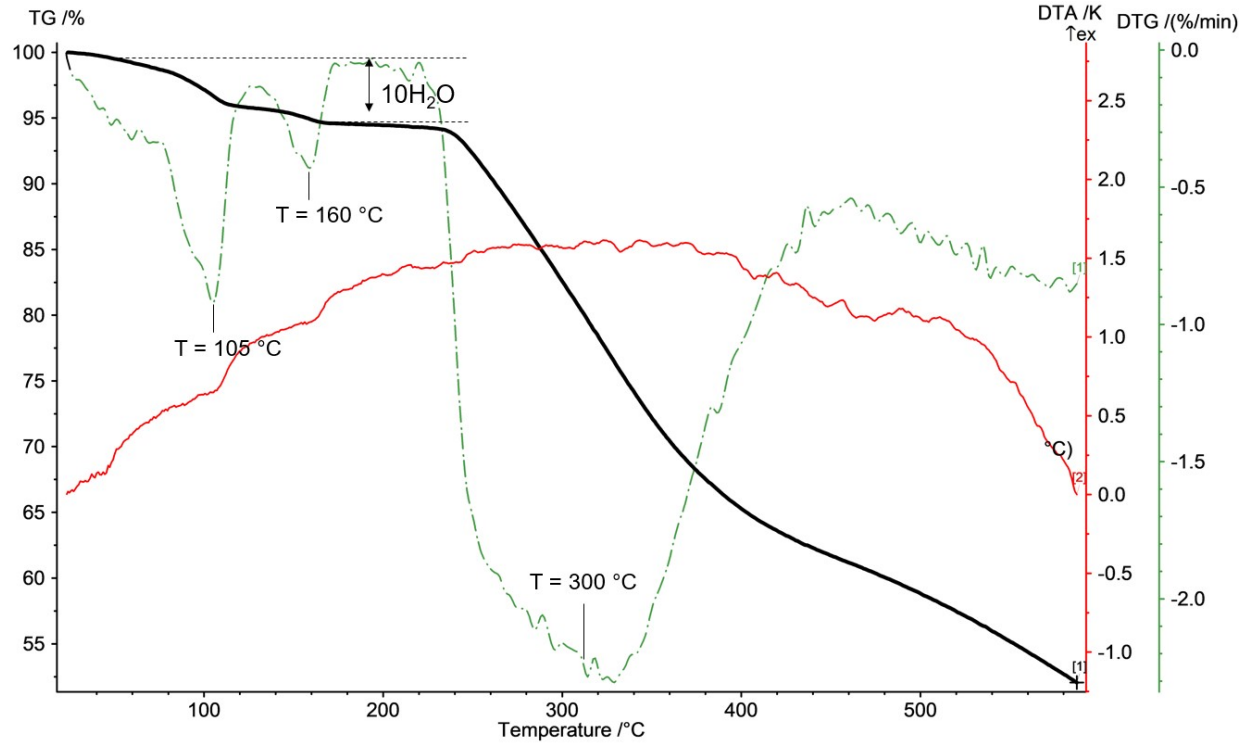

Figure S6. The thermogravimetric curve of compound $\mathbf{2}^{\mathbf{Tb}}$.

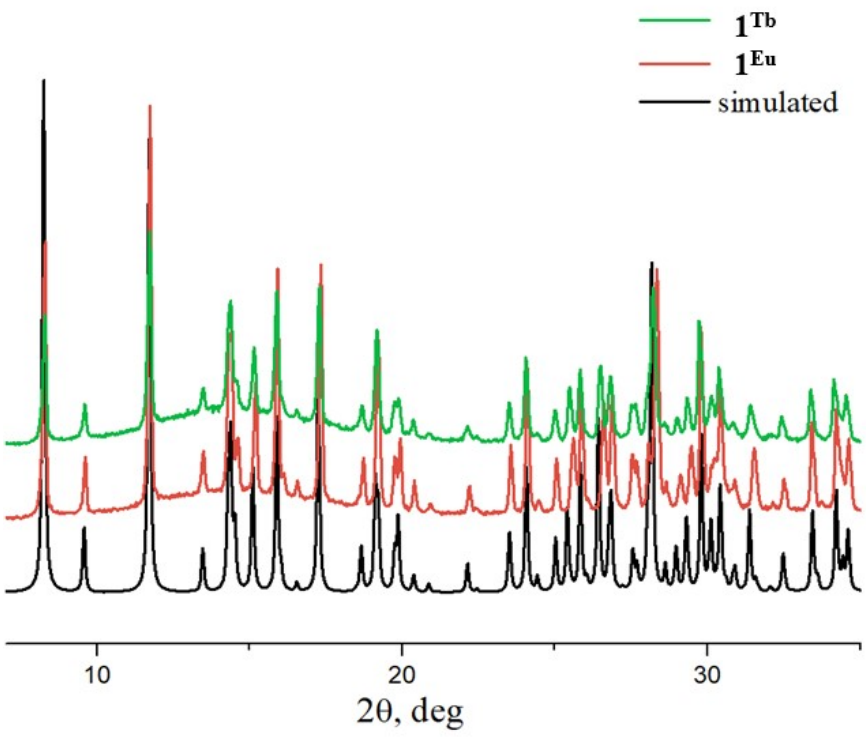

a)

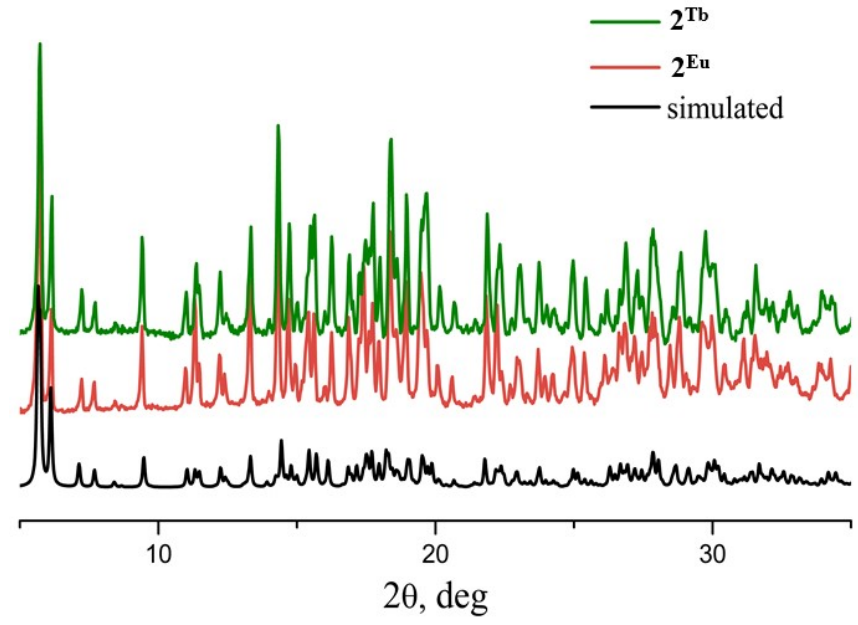

b)

Figure S7. The experimental and simulated patterns: (a) for the coordination polymers $\mathbf{1}^{Eu}$ and $\mathbf{1}^{Tb}$; (b) for the hexanuclear complexes $\mathbf{2}^{Eu}$ and $\mathbf{2}^{Tb}$.

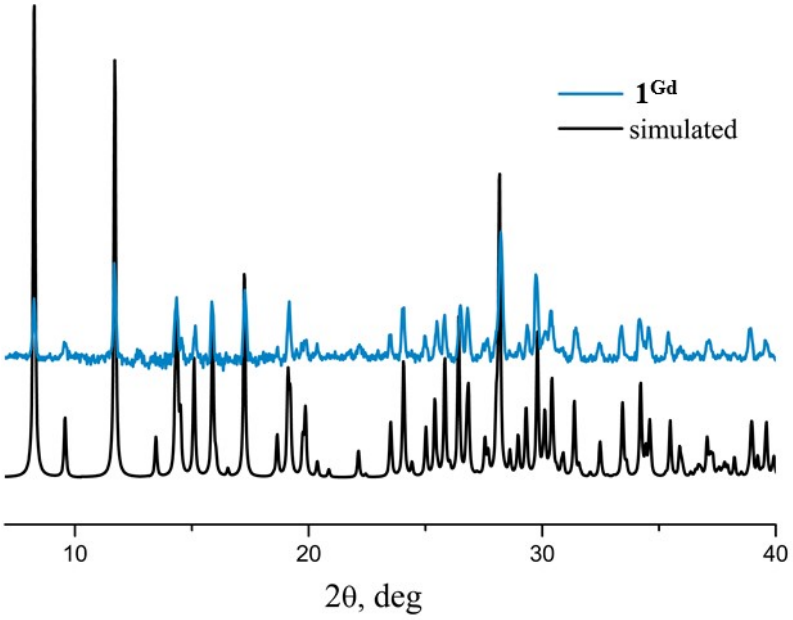

Figure S8. The experimental (**1**^{Gd}) and simulated (**1**^{Eu}) powder X-ray diffraction patterns of the coordination polymers.

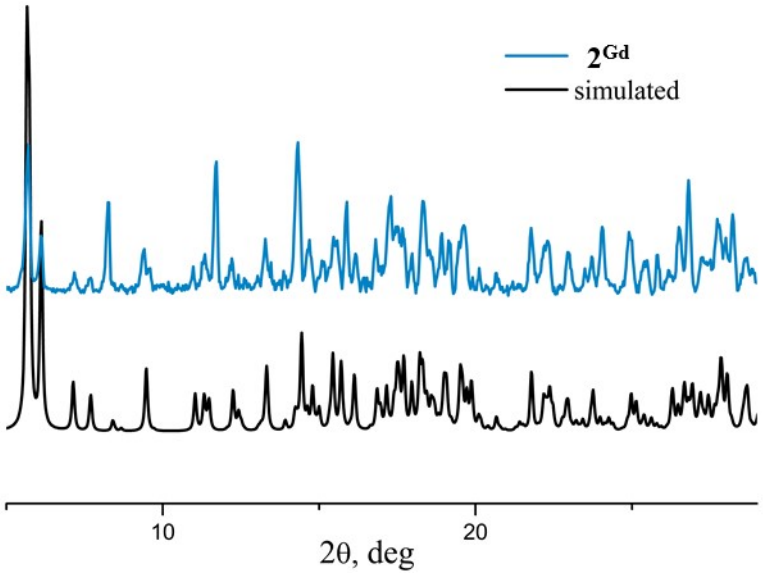

Figure S9. The experimental (**2**^{Gd}) and simulated (**2**^{Eu}) powder X-ray diffraction patterns of the hexanuclear compounds.

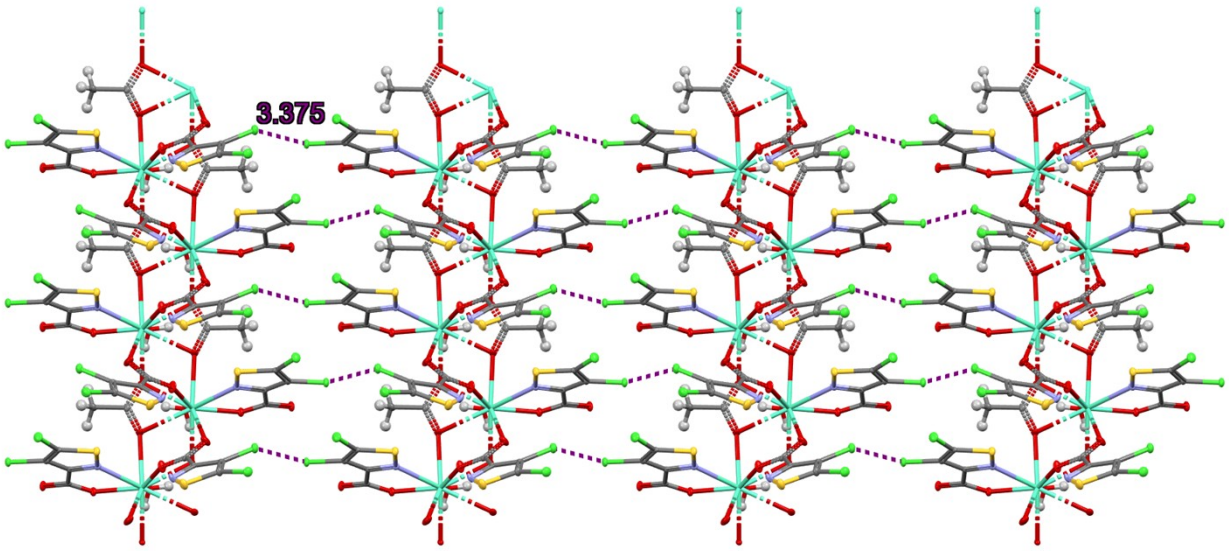

Figure S10. The non-covalent Cl···Cl interactions in complex $\mathbf{1}^{\mathbf{Eu}}$.

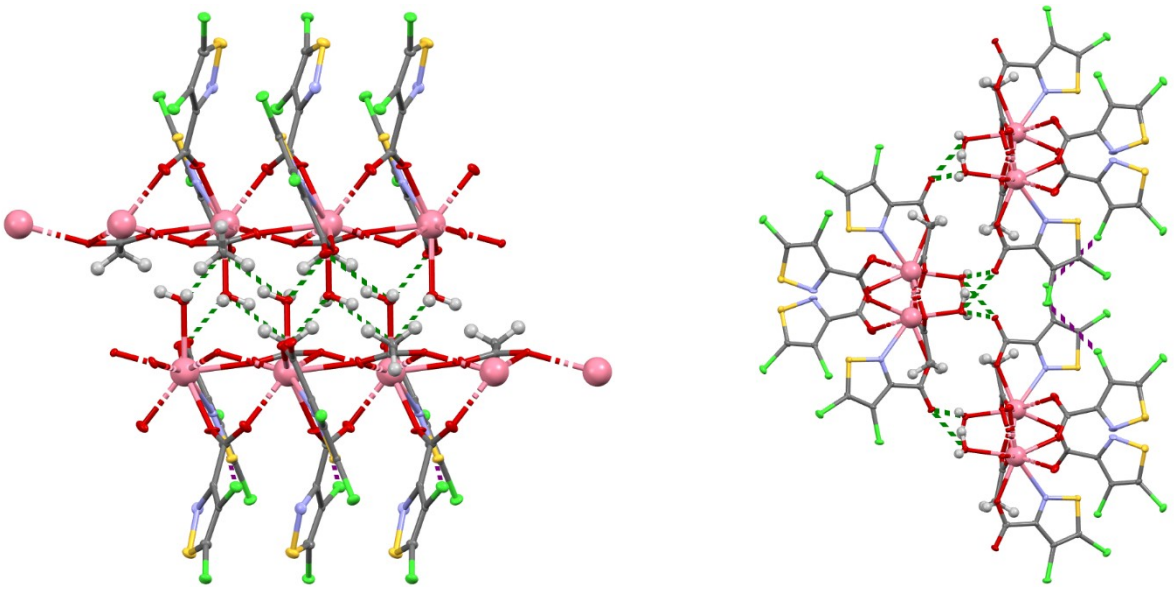

a) b)

Figure S11. The intermolecular hydrogen bonds (green dotted lines) in complex $\mathbf{1}^{\mathbf{Eu}}$, view down crystallographic *a* (a) and *b* (b) axis. The purple dotted lines exhibit the Cl···Cl interactions.

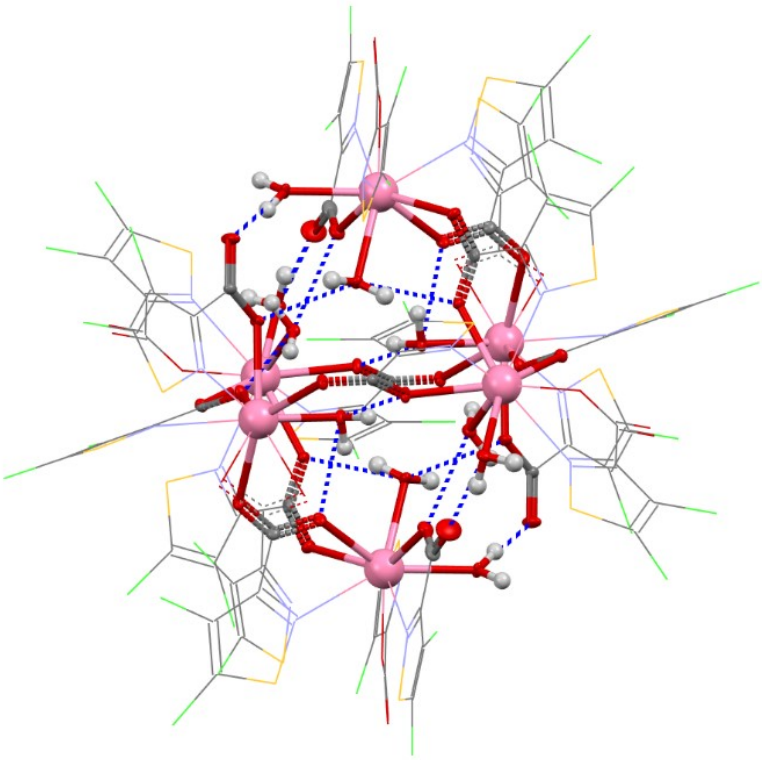

Figure S12. The intramolecular hydrogen bonds in hexanuclear complexes illustrated through **2**^{Eu}.

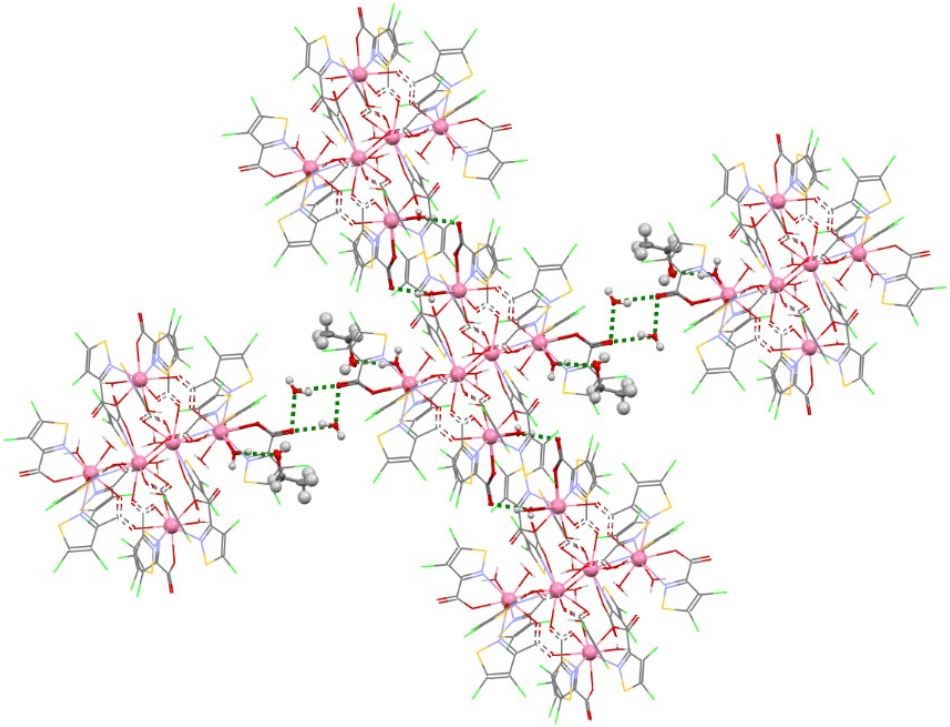

Figure S13. The intermolecular hydrogen bonds in hexanuclear complexes illustrated through **2**^{Eu}.

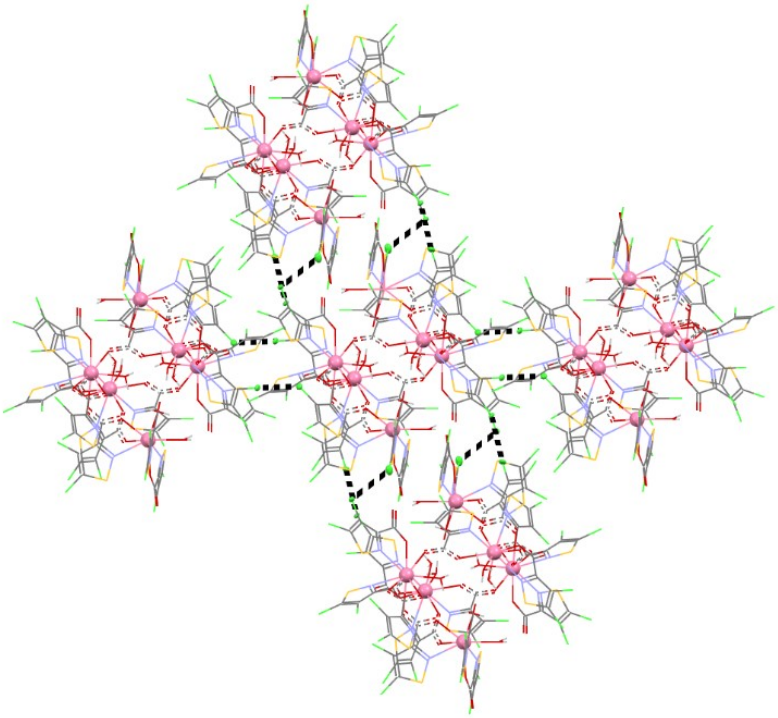

Figure S14. The non-covalent Cl···Cl interactions in hexanuclear complexes illustrated through **2**^{Eu}.

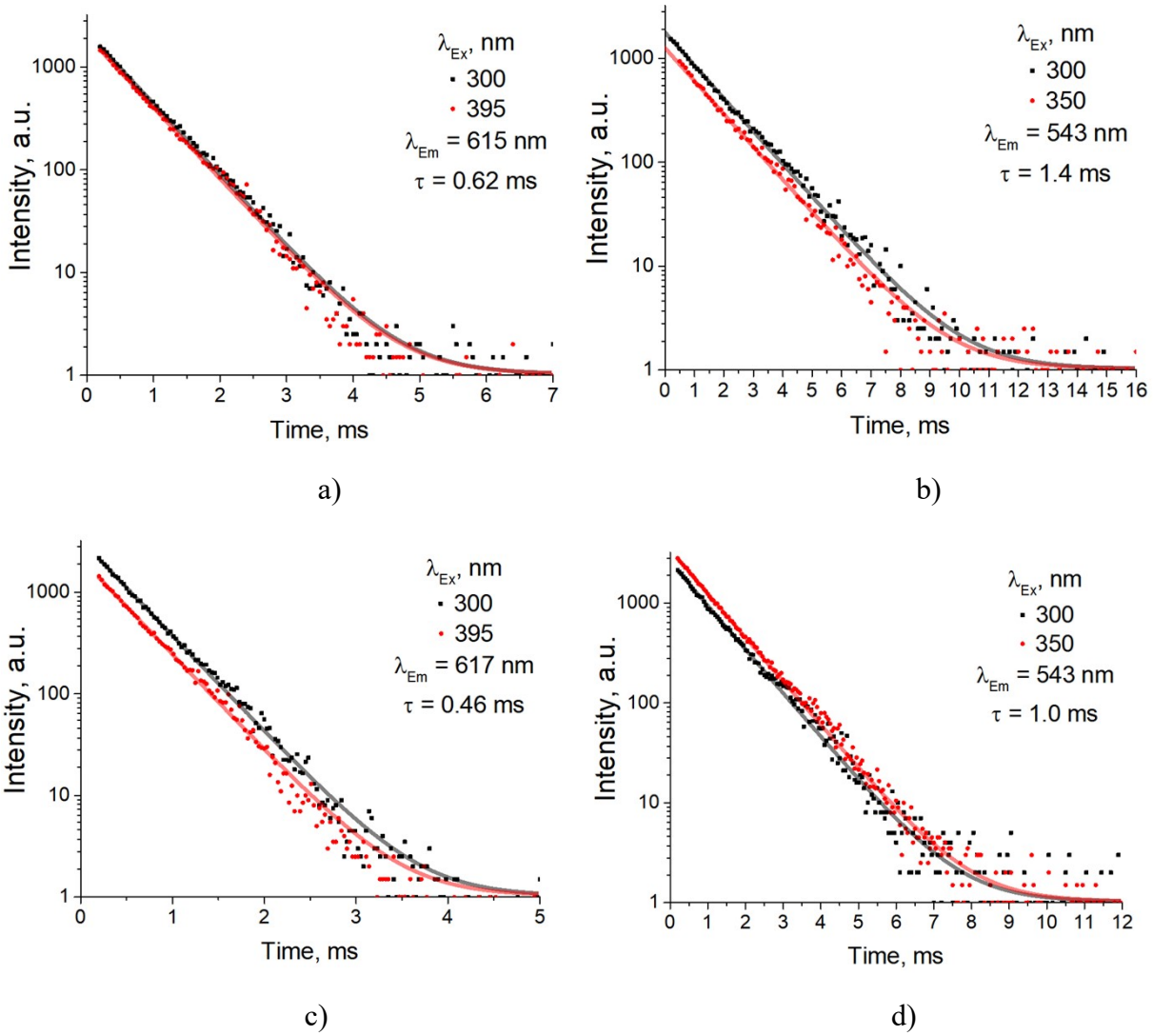

Figure S15. Luminescence kinetics at two wavelengths: a) 1^{Eu}, b) 1^{Tb}, c) 2^{Eu} and d) 2^{Tb}.

Table S1. The Ln–O and Ln–N bond lengths in complexes, the distances between oxygen atoms in intra- and intermolecular hydrogen bonds, as well as distances between chlorine atoms in non-covalent interactions.

Complex	1^{Eu}	2^{Eu}	2^{Tb}
Ln–O(L), Å	2.337(5) 2.365(5) 2.425(6)	2.393(3) 2.459(3) 2.448(4) 2.426(3) 2.472(3) 2.451(3)	2.404(4) 2.377(3) 2.432(3) 2.447(3) 2.411(4) 2.453(4)
		2.409(3) 2.408(3) 2.369(3) 2.422(3)	2.381(3) 2.352(3) 2.388(3) 2.419(3)
		2.418(3) 2.355(3) 2.374(3) 2.432(4)	2.402(3) 2.332(3) 2.417(3) 2.351(3)
Ln–N(L), Å	2.609(6)	2.547(4) 2.742(4)	2.529(4) 2.720(4)
		2.634(4) 2.653(4) 2.606(4)	2.616(4) 2.625(4) 2.583(4)
		2.703(4) 2.635(4) 2.673(4)	2.700(4) 2.606(4) 2.638(4)
Ln–O(OAc^-), Å	2.560(6) 2.451(5) 2.485(5) 2.549(5)	–	–
Ln–O(H_2O), Å	2.426(5)	2.381(3)	2.355(3)
		2.426(4) 2.400(3)	2.376(3) 2.387(4)
		2.420(4) 2.350(3)	2.381(3) 2.317(3)
O···O_{intra}, Å	–	2.584 2.670 2.713 2.653 2.747 2.669 2.772 2.814	2.648 2.690 2.745 2.697 2.580 2.763 2.803 2.669
O···O_{inter}, Å	2.733 2.807	2.814 2.895 2.926 2.668	2.902 2.947 2.657
Cl···Cl, Å	3.375	3.409 3.389 3.464	3.406 3.395 3.443

Table S2. Crystallographic data of the ligand and complexes.

Identification code	**1^{Eu}**	**2^{Eu}**	**2^{Tb}**
Empirical formula	$C_{10}H_5Cl_4EuN_2O_7S_2$	$C_{76}H_{36}Cl_{36}Eu_6N_{18}O_{50}S_{18}$	$C_{78}H_{43.6}Cl_{36}N_{18}O_{51.8}S_{18}Tb_6$
Formula weight	623.04	4766.27	4868.48
Crystal system, space group	Orthorhombic, *Pbca*	Triclinic, *P-1*	Triclinic, *P-1*
a/Å	13.1427(15)	15.1212(5)	15.1127(9)
b/Å	7.0058(8)	15.7752(5)	15.7212(8)
c/Å	36.927(4)	16.1319(5)	16.1012(8)
α/°	90	83.3690(10)	83.437(2)
β/°	90	73.4220(10)	73.608(2)
γ/°	90	83.5580(10)	83.519(2)
Volume/Å^3	3400.0(7)	3650.8(2)	3632.9(3)
Z	8	1	1
ρ_{calc} g/cm^3	2.434	2.168	2.156
μ/mm^{-1}	4.602	3.541	3.885
Crystal size/mm	0.065 × 0.015 × 0.01	0.085 × 0.065 × 0.04	0.05 × 0.04 × 0.025
2Θ range for data collection/°	3.804 to 52.746	3.678 to 58.282	3.558 to 54.216
Index ranges	$-15 \le h \le 16$, $-7 \le k \le 8$, $-46 \le l \le 41$	$-19 \le h \le 20$, $-20 \le k \le 21$, $-21 \le l \le 22$	$-19 \le h \le 19$, $-20 \le k \le 19$, $-20 \le l \le 20$
Reflections collected	15409	44085	15985
Independent reflections	3478 [R_{int} = 0.0988, R_{sigma} = 0.1055]	19515 [R_{int} = 0.0658, R_{sigma} = 0.1128]	15985 [R_{int} = 0.0813, R_{sigma} = 0.0528]
Restraints / parameters	0 / 237	1 / 931	2 / 904
Goodness-of-fit on F^2	0.991	0.942	1.041
Final R indexes [I>=2σ (I)]	R_1 = 0.0450, wR_2 = 0.0936	R_1 = 0.0484, wR_2 = 0.0703	R_1 = 0.0395, wR_2 = 0.0916
Final R indexes [all data]	R_1 = 0.0824, wR_2 = 0.1121	R_1 = 0.0930, wR_2 = 0.0808	R_1 = 0.0575, wR_2 = 0.0968
Largest diff. peak/hole / e/Å^{-3}	0.96 / -0.99	1.34 / -1.14	1.80 / -1.07
CCDC	2379781	2379782	2379783